

1 **Sedimentary response to sea-ice and atmospheric**
2 **variability over the instrumental period off Adélie Land,**
3 **East Antarctica**

4
5 **Campagne, P.^{1,2,3,4}, Crosta, X.¹, Schmidt, S.¹, Houssais, M. N.², Ther, O.¹, and**
6 **Massé, G.^{2,3}**

7 [1]{EPOC, UMR CNRS 5805, Université de Bordeaux, Allée Geoffroy St Hilaire, 33615
8 Pessac, France}

9 [2]{LOCEAN, UMR CNRS/UPCM/IRD/MNHN 7159, Université Pierre et Marie Curie, 4
10 Place Jussieu, 75252 Paris, France}

11 [3]{TAKUVIK, UMI 3376 UL/CNRS, Département de Biologie, Université Laval, G1V 0A6
12 Quebec (Quebec), Canada}

13 [4]{Québec-Océan, Université Laval, 1045 Avenue de la Médecine, G1V 0A6 Quebec
14 (Quebec), Canada}

15
16 Correspondence to: P. Campagne (p.campagne@epoc.u-bordeaux1.fr)

17
18 **Abstract**

19 Diatoms account for a large proportion of primary productivity in Antarctic coastal and
20 continental shelf zones. Diatoms, which have been used for a long time to infer past sea-
21 surface conditions in the Southern Ocean, have recently been associated with diatom specific
22 biomarkers (HBI). Our study is of the few sedimentary research projects on diatom ecology
23 and associated biomarkers in the Antarctic seasonal sea-ice zone. To date, the Adélie Land
24 region has received little attention, despite evidence for the presence of high accumulation of
25 laminated sediment, allowing for finer climate reconstructions and sedimentary process
26 studies. Here we provide a sequence of seasonally to annually laminated diatomaceous
27 sediment from a 72,5 cm interface core retrieved on the continental shelf off Adélie Land,
28 covering the 1970-2010 C.E. period. Investigations through statistical analyses of diatom

29 communities, diatom specific biomarkers and major element abundances document the
30 relationships between these proxies at an unprecedented resolution. Additionally, comparison
31 of sedimentary records to meteorological data monitored by automatic weather station and
32 satellite derived sea-ice concentrations help to refine the relationships between our proxies
33 and environmental conditions over the last decades. Our results suggest a coupled interaction
34 of the atmospheric and sea-surface variability on sea-ice seasonality, which acts as the
35 proximal forcing of siliceous productivity at that scale.

36

37 **1 Introduction**

38 Diatoms have been long time used to infer past sea-surface conditions in the Southern Ocean
39 on the basis of large-scale ecological studies from the plankton (e.g. Hasle, 1969) and surface
40 sediments (DeFelice and Wise, 1981; Zielinski et al., 1997; Armand et al., 2005; Crosta et al.,
41 2005). However, little is known about diatom ecology in the seasonal sea-ice zone and,
42 especially, in the coastal and continental shelf zone (CCSZ) off East Antarctica. The Adélie
43 Land region has especially received little attention despite evidence about high accumulation
44 sites of laminated sediments (e.g. Escutia et al., 2010). A very limited number of ecological
45 studies have been performed at the species or species group level in the plankton (Beans et al.,
46 2008; Riaux-Gobin et al., 2013) or sediments (Leventer et al., 1992; Maddison et al., 2006,
47 2012; Denis et al., 2006), and even fewer studies have investigated their relationships with
48 local or regional environmental conditions. As a result, diatom-based paleoenvironmental
49 reconstructions for this area are derived from large scale studies and do not take into account
50 the regional specificities. The Adélie Land region is of further particular interest due to the
51 presence of coastal polynyas, in the vicinity of the Dumont d'Urville station (DDU) and the
52 Mertz Glacier (MG), that are biologically very productive and where intense sea-ice
53 formation during winter leads to a large volume of dense water production (Arrigo and van
54 Dijken 2003; Sambrotto et al. 2003; Laccara et al., 2014) fueling the global circulation
55 (Rintoul et al., 1998).

56 Investigations of diatom communities, diatom specific biomarkers and major element
57 concentrations at high resolution along a 72.5 cm long interface core retrieved in the Dumont
58 d'Urville Trough (DDUT) allowed documentation of the relationships between these proxies.
59 Additionally, the comparison of our proxy records to meteorological data inferred from DDU
60 automatic weather station and satellite derived sea-ice concentrations helped to determine the

61 relationships between environmental conditions and proxy data, and consequently, the
62 sedimentary response to atmospheric and sea-surface changes. Here, we refine our knowledge
63 of diatom ecology at the regional scale and propose a robust tool to infer past sea-surface
64 conditions off Wilkes Land.

65

66 **2 Environmental settings**

67 **2.1 Geographic features**

68 The DDUT (Fig. 1b), located along the Adélie Land on the East Antarctic margin is
69 composed of several glacial depressions. These topographic features, up to 1,000 meters deep,
70 act as traps for sedimentary material (primary production and terrigenous particles) settling
71 out from surface waters. The trough runs from the front of the Zélée and Astrolabe glaciers to
72 the continental shelf break along a SE-NW orientation, and is bordered on its eastern side by
73 the Dumont D'Urville Bank (DDU Bank; Fig. 1b), which culminates at 200 meters below sea
74 level and limits exchanges with the Adélie Depression. On the western side, the DDUT is
75 flanked by the Dibble Bank where the Dibble Ice Tongue perdures during summer as a
76 seaward protrusion.

77

78 **2.2 Water masses**

79 The Adélie Land is influenced by several water masses and currents (Rintoul et al., 1998;
80 Williams and Bindoff, 2003; Williams et al., 2008). The wind-driven East Wind Drift flows
81 westward at the surface, and transports Antarctic Surface water that constitutes the summer
82 sub-surface water mass on the continental shelf. The Circumpolar Deep Water upwells near
83 the Antarctic Divergence and intrudes onto the plateau during summer. The High-Salinity
84 Shelf Water originates from brine rejections during winter sea-ice formation and from the
85 winter cooling of the Circumpolar Deep Water (Fig. 1). The High-Salinity Shelf Water flows
86 northward at the sea-floor as part of the dense shelf waters, here Adélie Land Bottom Water,
87 which represents a major contributor to Antarctic Bottom Water (Rintoul et al., 1998; Jacobs
88 et al., 2004; Meredith et al., 2013).

89

90 **2.3 Wind conditions**

91 The Adélie Land coast experiences the windiest conditions ever recorded on Earth through
92 the presence of intense katabatic winds (Périard and Pettré, 1993) that are funneled by narrow
93 glacial valleys close to the shoreline (Wendler et al., 1997). Although relatively strong winds
94 (>10 m/s) blow widely between 65° and 225° at DDU, the station is characterized by a
95 dominant and recurrent katabatic wind from 140°-180° (SE) coinciding with maximum wind
96 speeds (> 25 m/s) (Adolph and Wendler, 1995; Koning-Langlo et al., 1998). Such winds
97 support the annual occurrence of polynyas in the region, such as the DDU Polynya (DDUP;
98 66.11°S–139.31°E), where important sea-ice production occurs (Adolphs and Wendler, 1995;
99 Massom et al., 1998; Arrigo and van Dijken 2003).

100

101 **2.4 Sea-ice conditions**

102 In general, the sea-ice melts every year between November/December and reforms in
103 February/March, with sea-ice concentrations greater than 80% in winter and dropping below
104 20% in summer (Arrigo and van Dijken, 2003). Both pack ice and fast ice are observed in the
105 DDUT. Pack ice melts every year while fast ice may persist during summer months (Fig. 1a;
106 Massom et al., 2003; 2009; Smith et al., 2011; Wang et al., 2014). At its maximum extent,
107 fast ice develops ~100 km offshore between the Dibble Ice Tongue and the Adélie Bank (Fig.
108 1a; Massom et al., 2009; Smith et al., 2011). From the early spring to autumn, unstable fast-
109 ice conditions, characterized by several fast ice breakouts and re-formations as a result of lack
110 of anchor points, generally occur in the DDUT (Massom et al., 2009; Smith et al., 2011),
111 whereas fast ice persists later in the season over the banks. A key factor of the formation,
112 recurrence and persistence of these fast ice buttresses, are the numerous grounded small
113 icebergs on the Adélie and Dibble Banks that trap the passing pack ice and act as anchor
114 points for fast ice formation (Massom et al., 2001; Giles et al., 2008; Smith et al., 2011),
115 growing two ice promontories on either side of the core site. The presence of fast ice
116 buttresses is therefore closely associated to the intense sea-ice formation in the Mertz Glacier
117 Polynya and westward advection within the EDW (Fig. 1b; Massom et al., 2009).

118

119

120 **3 Material and Methods**

121 **3.1 Core description and ^{210}Pb chronology**

122 A 72.5 cm long interface core, DTCI2010, was retrieved aboard the R/V Astrolabe (66°24.68'
123 S; 140°26.67' E; 1010 m water depth) during the 2010 ALBION-HOLOCLIP cruise. Positive
124 X-ray images performed on the SCOPIX image-processing tool (Migeon et al., 1999) gave
125 detailed information about sediment density and structure. SCOPIX images revealed
126 laminations along the entire sedimentary section. The core was sampled continuously at 0.5
127 cm resolution and its chronological framework was determined based on ^{210}Pb excess ($^{210}\text{Pb}_{\text{xs}}$;
128 $T_{1/2} = 22.3$ years). The activities of ^{210}Pb and ^{226}Ra were measured on dried sediments by
129 non-destructive gamma spectrometry using a well-type, high efficiency low background
130 detector equipped with a Cryo-cycle (CANBERRA) (Schmidt and De Deckker, 2015).
131 Activities are expressed in mBq g⁻¹ and errors are based on 1 standard-deviation counting
132 statistics. $^{210}\text{Pb}_{\text{xs}}$ was determined by subtracting the activity supported by its parent isotope,
133 ^{226}Ra , from the total ^{210}Pb activity in the sediment. In the interface core DTCI2010, there is a
134 general downcore trend in decreasing $^{210}\text{Pb}_{\text{xs}}$ activities, from 242 to 74 mBq g⁻¹, as expected
135 due to the decay of the unsupported ^{210}Pb (Fig. 2). However, the observation of a layer where
136 activities decrease slowly between 10 and 40 cm led us to retain the Constant Initial
137 Concentration model (CIC; Robbins and Edgington, 1975) to calculate the age (t) of each
138 measured horizon as: $t = (1/\lambda) \ln (A_0/A_z)$ where t and A_z are the age of the sediment and the
139 excess ^{210}Pb activity at the depth z, A_0 is the activity at the surface and λ is the decay constant
140 of ^{210}Pb . This choice is supported by the almost constant activities measured in the uppermost
141 sediments of cores collected in 2003 (240 ± 13 mBq g⁻¹; Massé et al, 2011) and 2011 ($253 \pm$
142 13 mBq g⁻¹ in DTCI2011; Schmidt S., unpublished data). A second-order polynomial
143 function was calculated from the 11 ^{210}Pb -dates obtained over the entire core to build the age
144 model (Fig. 2).

145

146 **3.2 Sedimentary analyses**

147 **3.2.1 Diatoms**

148 Micropaleontological analyses were performed according to the methodology described in
149 Rathburn et al. (1997) at a ~0.25 year resolution (every 0.5 cm) in core DTCI2010. Counts

150 were performed under a microscope Olympus BH-2 at a magnification of x1000. For each
151 sample, 300-350 diatom valves were counted and data are presented as species relative
152 abundances. Diatom identification was performed to the species or species group level
153 following the taxonomical references detailed in Crosta et al. (2004) and the counting rules
154 described in Crosta and Koç (2007). Sixty-two diatom species were identified in down-core
155 assemblages, from which twenty-four presented abundances higher than 2% of the total
156 diatom assemblages (Table S1).

157 3.2.2 Biomarker

158 Few marine and freshwater diatoms belonging to *Haslea*, *Navicula*, *Pleurosigma* and
159 *Rhizosolenia* genera were recently found to be synthesizing Highly Branched Isoprenoids
160 (HBI) (Sinningh  Damst  et al., 2004; Mass  et al., 2011). Recent studies have proposed the
161 use of HBIs to reconstruct variations of Holocene Antarctic sea-ice duration as a
162 complementary approach to diatom counts (Collins et al., 2013; Campagne et al., 2015; Smik
163 et al., 2016). Biomarker analysis followed the technique described by Mass  et al. (2011) and
164 were also performed at a ~0.25 year resolution (every 0.5 cm) in core DTCI2010.

165 3.2.3 XRF

166 X Ray fluorescence (XRF) measurements were conducted on slab sections at a 2 mm
167 resolution along the entire core using an AAVATECH XRF core-scanner at two different tube
168 voltages (10 and 30 keV) allowing for the determination of major elements associated with
169 the detrital (Rubidium [Rb]) and terrigenous fractions (Zirconium [Zr] and Titanium [Ti]).
170 More details about the protocole can be found in Fleury et al. (2015).

171

172 3.3 Instrumental data

173 3.3.1 Atmospheric data

174 Daily measurements of wind direction (from 0 to 360 ), velocity (m/s) and temperature ( C)
175 for the time period 1956-2011 were obtained from the METEO France publith que. The
176 dataset is based on Automatic Weather Station at the DDU French station (66.7  S, 140  E;
177 Wendler et al., 1997), 30 km from the core site. The dataset provides monthly statistics based
178 on 6-hourly in-situ observations at 10 meters. Wendler et al. (1997) showed that from Penguin

179 Point (east of the Mertz Glacier) to DDU stations, meteorological parameters displayed
180 similar variations, leading to the conclusion that measurements from automatic weather
181 station were relatively robust. Wind direction represents the origin of the wind over 360°.
182 East/South/North/West -erly wind components indicate the number of days between
183 November and March during which the wind blows between 45°-135°/135°-225°/315°-
184 45°/225°-315° respectively. A ratio between easterly and southerly wind components
185 (hereafter noted E/S), and a ratio between northerly and westerly wind components (hereafter
186 noted N/W), were calculated and used to account respectively of the dominant and the
187 secondary wind directions in the region according litteratures and observations (Note S2).
188 Monthly anomalies are expressed relative to the mean value calculated for each month over
189 the 1979-2009 period.

190 3.3.2 Sea-ice data

191 Daily sea-ice concentrations (SIC) for the time period 1978-2012 were obtained from the
192 National Snow and Ice Data Center data repository. The dataset is based on passive
193 microwave observations from the Nimbus-7 SSMR (1978-1987) and DMSP SSM/I (1987-
194 2007) and SSMIS (2007-2012) radiometers processed with the NASA Team algorithm
195 (Cavalieri et al., 1995) at a spatial resolution of 25x25 km. Averaged sea-ice concentrations
196 (SIC) were calculated over the core site in the central part of the DDUT (Fig. S1). The sea-ice
197 retreat date was determined arbitrarily as the Julian day when the SIC (7-day average)
198 dropped below 40%, while the sea-ice advance corresponds to the day when SIC increased to
199 above 40%. The duration of the ice-free season corresponds to the number of days per year
200 during which SIC<40 %. Monthly anomalies are expressed relative to the mean value
201 calculated for each month over the 1979-2009 period.

202

203 3.4 Statistical analyses

204 Statistical analyses were run using the statistical software XLStat (Addinsoft). Principal
205 Component Analyses (PCA) and Pearson correlation tests (significance level $\alpha=0.05$) were
206 performed on all sixty-two diatom species including the species accounting for less than 1%
207 of the total diatom assemblage (Table S1), two diatom specific biomarkers along with their
208 associated ratio, three major elements including a ratio to, first (1) determine the relationships
209 between species and identify potential diatom cluster (in order to increase the statistical

210 weight of minor species) and (2) investigate the relationships between the different proxies in
211 our study. Complete statistical analyses are presented in Note S1 (Fig. S2; Table S2), and
212 allowed to identify the sedimentary proxies that are significant in our study area (presented in
213 Section 4), in terms of abundances and ecological preferences. Additionally in Note S2 (Fig.
214 S3; Table S3), PCA and the Pearson correlation test were performed on seasonally averaged
215 meteorological and satellite data to support the few previous oceanographic and atmospheric
216 observations about climate forcing and their environmental response in the area. This work
217 constituted a basis to a final PCA (presented in Section 5) between annually averaged
218 meteorological data and significant sedimentary proxies interpolated at one year, to
219 determine, through the sedimentary response, how the preserved signal respond to local
220 environmental parameters. Although the standardization of our data partially hide the
221 variability of our sedimentary signals (Fig. S4), the main characteristics are preserved and
222 allow for interannual comparisons.

223

224 **4 Results**

225 **4.1 Sedimentary signals**

226 The main diatom species and species groups identified in core DTCI2010 (Note S1) are
227 *Fragilariopsis cylindrus*, *Thalassiosira antarctica*, *Porosira glacialis* and *Porosira*
228 *pseudodenticulata* (hereafter noted *Porosira* gp; Note S1), *Fragilariopsis kerguelensis*, large
229 centric species (noted Open Water gp; Note S1), *Rhizosolenia* species (noted *Rhizosolenia* gp)
230 and *Chaetoceros Hyalochaete* resting spores (noted CRS). These diatom groups are presented
231 along with di-unsaturated HBI isomers [HBI:2], tri-unsaturated HBI isomers [HBI:3], and
232 their respective ratio, Titanium (Ti) contents and Zirconium versus Rubidium (Zr/Rb) that
233 constitute the main relevant geochemical proxies identified in our study area (Note S1). Other
234 diatom proxies such as the *Banquisia* gp, *Fragilariopsis obliquecostata*, *Fragilariopsis curta*,
235 *Eucampia antarctica*, the *Fragilariopsis* summer gp, the *Thalassiothrix* gp, *Fragilariopsis*
236 *rhombica*, *Chaetoceros Phaeoceros*, and the Benthic gp sometime used in the literature to
237 infer past sea-ice conditions are here not significant in term of population and/or relevant in
238 term of statistical relationships to other proxies and environmental parameters. They are
239 discussed in Note S1.

240 Highest abundances of *F. cylindrus* in sediments are observed during the ~1972-1979 C.E.,
241 1983-1984 C.E., 1996-1998 C.E. and 2002-2003 C.E. periods. [HBI:2] concentrations present
242 a similar pluri-decadal pattern to *F. cylindrus*. However, pluri-annual variations appear
243 opposite with higher concentrations in 1971-1978 C.E., ~1982 C.E., 1985-1986 C.E., ~1989
244 C.E., 1995-2002 C.E., and since 2006 C.E. (Fig. 3a). The CRS and Zr/Rb exhibit contrasting
245 trends during the 1970s to the mid 1980s, with decreasing CRS relative abundances and
246 increasing Zr/Rb values during the 1973-1976 C.E. and ~1977-1978 C.E. periods. They are
247 then relatively in phase with concomitant increasing values in 1984/1985-1987 C.E., and in
248 1989-1995 C.E. The Open Water gp and *F. kerguelensis* records display similar patterns,
249 increasing in 1972-1977 C.E., 1980-1986 C.E., 1995-2001 C.E. and ~2007 C.E. In the same
250 way, the Ti contents increase in 1975-1978 C.E., 1985-1987 C.E., 1996-2001 C.E. and
251 ~2008-2010 C.E.[HBI:3] and the *Rhizosolenia* gp exhibit similar pattern with high values in
252 ~1973-1975 C.E., moderate values in ~1978-1980 C.E., 1983-1985 C.E., and 1995-2001 C.E.
253 *Thalassiosira antarctica* increased slightly over the 1976-1978 C.E., 1982-1985 C.E. and
254 reached highest values between 2000-2010 C.E. The *Porosira* gp increased slightly over the
255 1980-1986 C.E. and large increases occurred around the ~2000 C.E. and 2007 C.E. periods.

256

257 **4.2 Environmental parameters**

258 Atmospheric data indicate the increasing occurrence of easterly winds from spring to autumn
259 (Fig. 3b) during the 1970-1975 C.E., 1983-1984 C.E., and between 1997-2007 C.E. periods
260 (Fig. 3b). At the opposite, southerly winds dominate during the 1976-1982 C.E., 1985-1996
261 C.E. periods and since 2008 C.E. (Fig. 3b). The increasing occurrence of northerly winds
262 from spring to autumn characterises the 1971-1975 C.E., 1979-1980 C.E., 1984 and 1992
263 C.E. and in the 1996-2001 C.E. periods, and more westerly winds occur between 1975-1979
264 C.E., 1981-1982 C.E., 1985-1991 C.E., 1993-1996 C.E., 2000 C.E. and since 2002 C.E. (Fig.
265 3b). Analysis of the satellite data reveals the presence of heavier sea-ice conditions in the area
266 during spring, summer and autumn in the 1979-1981 C.E., 1990-1998 C.E. and 2001-2004
267 C.E. periods (Fig. 3b), that coincide with delayed sea-ice retreat in spring-summer. At the
268 opposite earlier open conditions in spring occur between ~1981-1988 C.E., ~1994 C.E., ~1998-
269 2001 C.E. and ~2005-2007 C.E. (Fig. 3b). Delayed sea-ice advance in autumn characterises
270 the 1980s and the 2002 C.E. periods, while earlier sea-ice closing occur between 1989-2001
271 C.E. and since 2003 C.E. (Fig. 3b).

272

273 **5 Discussion**

274 Below, we first discuss the significance, behavior and relationships between the relevant
275 proxies at the DDUT site over the last 40 years. Secondly, we statistically confront 40 years
276 of instrumental records to our sedimentary signals, that are commonly used for paleoclimate
277 reconstructions, to refine our understanding of their ecological preferences or environmental
278 significance in the CCSZ at the regional scale of Adélie Land .

279

280 **5.1 Sedimentary signals off Adélie Land over the instrumental period**

281 • **Sea-ice proxies**

282 High occurrences of *F. cylindrus* populations and [HBI:2] in high-southern latitude water
283 column and sediments, including our study area, characterize spring sea-ice occurrence (Kang
284 and Fryxell, 1992; Armand et al., 2005; Massé et al., 2011; Smik et al., 2016; Table 1; Note
285 S1). High abundances of these proxies were used in Holocene sediments to track consolidated
286 sea-ice conditions lasting in summer (Leventer et al., 1993; Campagne et al., 2015). Our
287 results indicate that intervals characterised by heavier sea-ice conditions in the area during
288 spring to autumn (Fig. 3b) broadly coincide with those characterized by higher abundances of
289 *F. cylindrus* (Fig. 3a). However, changes in sea ice concentration do not satisfactorily explain
290 *F. cylindrus* variability during the last 40 years. Additionally, *F. cylindrus* abundances present
291 a weak agreement with the timing of the sea-ice retreat (Fig. 3). Conversely, a relation is
292 observed between *F. cylindrus* abundances and wind origin, where by increasing occurrences
293 of relatively weak northerly winds coincide with higher abundances of the species (Fig. 3). As
294 observed for *F. cylindrus*, changes in [HBI:2] concentration over the last 40 years do not
295 closely follow SIC variations nor seasonal sea-ice dynamics (Fig. 3). Rather, high
296 concentrations of this biomarker co-occur with more westerly winds (Fig. 3).

297 *Thalassiosira antarctica* and the *Porosira* gp were found to share similar seasonal occurrence
298 in autumn, although it has been suggested that *P. glacialis* prefers slightly colder and icier
299 conditions (Pike et al., 2009; Table 1; Note S1). *Thalassiosira antarctica* and the *Porosira* gp
300 have thus been interpreted in Holocene sediments to indicate a late summer/autumn rapid
301 deposition, linked to early sea-ice return (Denis et al., 2006; Maddison et al., 2006, 2012). As

302 already observed for previous sea-ice related proxies, the distribution of autumnal bloom
303 species does not closely follow SIC variations in our study area (Fig. 3). However, our results
304 suggest that the occurrence *T. antarctica* and the *Porosira* gp should be linked to sea-ice
305 dynamics and wind variability, as large increase of *T. antarctica* and *Porosira* gp over the
306 2000s coincides with the earliest sea-ice advance in the last 30 years and the prevalence of
307 easterly winds (Fig. 3).

308

309 • **Open ocean proxies**

310 Along with the Open Water gp, *F. kerguelensis* was found to dominate the summer-autumn
311 laminae off East Antarctica and record a lengthening of the open water season and a warming
312 of sea-surface waters in summer (Denis et al., 2006; Maddison et al., 2006; Table 1; Note S1).
313 In our data, open ocean proxies seem to follow regional sea-ice conditions relatively well,
314 regardless the sea-ice origin, structure and nature. Indeed, the Open Water gp and *F.*
315 *kerguelensis* present highest relative abundances (Fig. 3a) during periods of low SIC, earlier
316 sea-ice retreat and enhanced ice free season (Fig. 3b) and lowest values during periods of
317 heavier sea-ice conditions.

318 Ti content in sediment is an indicator of open water conditions (Table 1; Note S1), mainly
319 reflecting variations in terrigenous delivery by glacial melting (Presti et al., 2003; Escutia et
320 al., 2003). In our records, the Ti pattern is relatively coherent with the Open Ocean gp and *F.*
321 *kerguelensis* records (Fig. 3a). Highest values generally occur during low SIC periods, long
322 ice free seasons and high temperatures such as during the 1980s. However, some
323 discrepancies occur as highest sedimentary Ti values in 1970-1972 C.E. are concomitant to
324 only a slight increase of open ocean proxies and no particular warming event in monitored
325 temperatures (Fig. 3). This suggests that Ti content can be impacted by rapid deposition
326 events that are independent of the length or the warmth of the ice-free season. Therefore,
327 downcore differences between Ti and open ocean proxies may help identifying episodic
328 processes such as local glacial discharge or ice rafted material derived from the Mertz Glacier
329 Tongue basal melting (Maddison et al., 2006; Dinniman et al., 2012; Campagne et al., 2015).

330 [HBI:3] have been identified in water column phytoplankton (Massé et al., 2011; Table 1;
331 Note S1), synthesized by the Rhizosolenoids (Sinningh Damsté et al., 2004). The latter
332 diatom group is generally associated to late summer season production and to long diatom

333 productivity season, linked with turbulent open ocean conditions (Armand et al. 2005; Crosta
334 et al. 2005; Beans et al., 2008; Note S1). In core DTCI2010, [HBI:3] and the *Rhizosolenia* gp
335 display similar patterns, and present a strong relation with ice-free conditions (Fig. 3b). The
336 maximum occurrence of [HBI:3] between the mid 1970s to the mid 1980s coincides well with
337 positive temperature anomalies and lower wind speed anomalies at that time (Fig. 3b),
338 arguing for a strong relationship between the biomarker development and surface conditions
339 forced by atmospheric variability.

340

341 • **Polynya activity proxies**

342 High percentages of CRS in Holocene sediments from AGVL have been associated to strong
343 siliceous productivity supported by melting ice-induced stratified surface waters and strong
344 intermittent surface mixing conditions (Maddison et al., 2006; Table 1; Note S1). Off Adélie
345 Land, vertical mixing along with variations in bottom current velocities were associated to
346 enhanced polynya activity (Campagne et al., 2015; Table 1; Note S1), and were estimated
347 from changes in sediment grain size inferred the Zr/Rb ratio relative abundances. In core
348 DTCI2010, CRS and Zr/Rb exhibit contrasting trends during the 1970s to the mid 1980s, but
349 are then relatively in phase over the last 20 years (Fig. 3a). Zr/Rb follows SIC variations
350 relatively well whereas CRS relative abundances seem to follow spring sea-ice dynamics
351 (Fig. 3). Interestingly, a relationship is observed between CRS abundances and Zr/Rb with
352 wind pattern, as both proxies coincide well with the prevalence of southerly winds in our
353 study area, e.g. between 1983-1996 C.E. (Fig. 3), arguing for a strong relationship between
354 the polynya activity and atmospheric pattern variability.

355

356 **5.2 The coupled role of wind pattern and sea-ice variability on sea surface** 357 **productivity in Adélie Land**

358 PCA between seasonal atmospheric forcing and sea-ice conditions over the core site (Note
359 S2; Fig. S3) argues that wind conditions, and particularly wind direction, exert a strong
360 impact on sea-surface conditions off Adélie Land, in agreement with several studies at larger
361 spatial scales (Massom et al., 2003; 2009; Smith et al., 2011; Wang et al., 2014; Campagne et
362 al., 2015). Based on PCA analyses between our proxy records and instrumental data, we
363 document the sedimentary response to changes in environmental conditions with a special

364 emphasis on wind fields and wind induced sea-ice variability and, therefore, we refine proxies
365 validation at the regional scale (Note S2; Fig. S3; Table S3). Results are summarized and
366 presented in Table 1.

367 Here, environmental parameters were averaged over the ice-free season (from November to
368 March) to allow a direct comparison of the impact of atmospheric and sea-surface conditions
369 on the sedimentary response, and by inference, on the biological surface response. F1 axis,
370 which accounts the highest variance of 18.09 % (Fig. S5), represents sea-ice conditions from
371 November to March, as driven by SIC, the length of the sea-ice free season and the sea-ice
372 dynamics (Fig. 4). The easterly wind direction is significant on F1+ while the southerly wind
373 component is significantly located on F1- (Fig. 4; Table S4), indicating that sea-ice conditions
374 and dynamics off Adélie Land are strongly impacted by the dominant wind field. F2 axis
375 accounts for 16 % of the total variance (Fig. S5). Westerly and northerly wind directions are
376 significantly located on F2- and F2+, respectively, with very low scores on F1 (Fig. 4; Table
377 S4). Increasing wind direction (southerly to westerly winds) or weak onshore (northerly
378 winds) circulation is of cyclonic origin in our study area (Heil et al., 2006; Parish and
379 Bromwich, 2007; Wang et al., 2014). This result suggests that storm forcing on sea-ice
380 conditions are represented by the F2 axis. We hereafter present the sedimentary response to the
381 four cases of mean wind fields and wind-induced sea-ice conditions identified by our PCA
382 analyses (Note S2; Fig. S3).

383

384 • **Westerly winds increase spring sea-ice conditions**

385 A dominant westerly wind component originating from enhanced cyclone activity conducts to
386 lower temperatures and wind speed in our data (Heil et al., 2006; Parish and Bromwich, 2007;
387 Massom et al., 2003; 2009; Wang et al., 2014; Note S2). Westerly winds have been observed
388 to decrease the open water fraction, promote pack ice or thinner sea ice lasting longer in
389 spring and delayed sea-ice advance in autumn in our study area (Massom et al., 2003; Heil et
390 al., 2006; Smith et al., 2011; Wang et al., 2014; Zhai et al., 2015; Note S2). Under such
391 conditions, the sedimentary response shown by the PCA indicates increased content of the
392 [HBI:2]/[HBI:3] ratio, which is significantly correlated with westerly winds (0.398; Table S4)
393 and presents a strong negative relationship with low temperature in our data (Fig. 4). Similar
394 relationships are observed for [HBI:2] (Fig. 4). Our observations agree with the
395 environmental interpretation these proxies as sea-ice and cold environment indicators (Table

396 1; Note S1). Indeed, it has been suggested recently that relatively high [HBI:2] in surface
397 samples from East Antarctica might be a good indicator of extended (into summer) seasonal
398 sea-ice cover, whereas melt-water stratified marginal sea-ice environments should be
399 associated with lower [HBI:2] (Smik et al., 2016). Therefore, the occurrence of [HBI:2] in
400 sediments might attest the presence of overlying heavy pack-ice conditions or episodic fast
401 ice presence, in spring to summer time in our study area (Table 1).

402

403 • **Northerly winds increase spring sea-ice conditions**

404 At the Antarctic scale, northerly winds promote early spring sea-ice retreat and late autumn
405 sea-ice advance (Stammerjohn, et al., 2008). However, northerly winds in our study area have
406 been observed to decrease northward transport of sea ice and increases sea-ice duration
407 (Holland et al., 2012; Wang et al., 2014). Our PCA results (Fig. 4) indicate that the northerly
408 wind component is associated with lower wind speeds conducive to delayed sea-ice advance
409 at the core site (Note S2), but relationships with SIC and sea-ice retreat date are not clear in
410 our data. We here propose that northerly winds have two opposite impacts on sea-ice
411 conditions off Adélie Land. First, they tend to increase spring sea-ice presence in the area,
412 likely by pushing the offshore pack ice toward the coast or limiting its northward transport.
413 Secondly, they contribute to increase summer melting and delay ice regrowth in autumn by
414 transporting warm air from the north and by enhancing the swell. Under such environmental
415 conditions, the sedimentary response shown by the PCA indicates increasing abundances of
416 the *Rhizosolenia* gp, [HBI:3] and *F. cylindrus*, that have high scores on F2+ (Fig. 4). The
417 concomitant presence of sea-ice related proxies and open ocean proxies indicate a marked
418 seasonal cycle. *Fragilariopsis cylindrus* displays a strong association with high temperature in
419 our study area, but present a non-significant positive relationship with SIC (Table S4). Our
420 results may thus indicate that *F. cylindrus* respond to pack-ice presence in spring and
421 subsequent rapid melting (Table 1) as previously evidenced elsewhere (Gersonde and
422 Zielinski, 2000; Armand et al., 2005).

423 Our results suggest that both *F. cylindrus* and [HBI:2] are associated with longer sea-ice
424 duration in spring/summer in our study area (Table 1). They however respond to different sea-
425 ice conditions whereby sea-ice dwelling diatoms synthesizing the [HBI:2] have greater
426 affinities with heavy pack-ice or fast-ice conditions under more westerly winds (colder sea
427 ice) while *F. cylindrus* develops at the pack-ice edge and within sea-ice meltwater conditions

428 under weak northerly winds (warmer sea ice) (Table 1). This dichotomy may explain that the
429 biomarker record lags the diatom record by ~2 years in core DTCI2010 (Fig. 3a). However,
430 time series studies on the formation, export and burial of HBIs and diatoms are necessary to
431 fully understand this decoupling. We note that [HBI:2] and *F. cylindrus* present similar trends
432 at decadal to pluri-decadal scales, supporting their use as complementary sea-ice indicators
433 for paleoclimate studies (e.g. Campagne et al., 2015). Regarding the productivity associated
434 to summer time, the presence of [HBI:3], a marker of open water related productivity, along
435 with *Rhizosolenia* gp, an indicator of warmer conditions and of a long diatom productivity
436 season (Note S1), would support the presence of stable sea-surface conditions due to low
437 wind speed during summer and of enhanced open water conditions in autumn (Table 1).

438

439 • **Easterly winds induce open conditions**

440 A dominant easterly wind component yields to earlier sea-ice retreat and earlier sea-ice
441 advance, lower SIC from November to March and, in some extent, to a longer ice-free season
442 in the study area (Fig. 4; Note S2). Easterly winds tend to increase ice advection and icebergs
443 in the area and contribute to building a fast-ice buttress over the banks (Massom et al., 2009).
444 Persistence of fast-ice promontories during the summer over the Dibble and the DDU banks,
445 can in turn acts as a barrier to westward sea-ice advection and leads to the establishment of
446 open water conditions over the DDUT, as observed in several locations off East Antarctica
447 (e.g. MGP and Terra Nova Bay polynyas) (Arrigo and van Dijken, 2003; Massom et al., 2001;
448 2009; Campagne et al., 2015). Similarly in autumn, easterly winds tend to increase ice
449 advection and icebergs in the area, providing favourable conditions for the formation of thick
450 fast ice and buttress earlier in the autumn (Heil et al., 2006). Under such environmental
451 conditions, the PCA indicates that the sedimentary response consists of higher abundances of
452 several proxies strongly inter-correlated on F1+, *T. antarctica*, the *Porosira* gp, *F.*
453 *keruelensis*, [HBI:3] and Ti (red shaded area on Fig. 4; Table S4). The Ti signal is also
454 linked to the northerly wind component (Table S4), suggesting that this proxy is tied to
455 onshore wind circulation and probably responds to longer ice free season. *Thalassiosira*
456 *antarctica*, *Porosira* gp, *F. kerguelensis* and Ti are strongly linked to low SIC over the ice-
457 free season in our study area (Table S4). Similarly, [HBI:3], the *Porosira* gp (-0.431; Table
458 S4), *F. kerguelensis* (-0.360) and *T. antarctica* are strongly associated with earlier open water
459 conditions, and *F. kerguelensis* is linked to a longer ice-free season. We conclude that the

460 Open Water gp, *F. kerguelensis*, Ti and [HBI:3] are associated with long ice-free seasons
461 associated to easterly winds, suggesting that these species develop under oligotrophic and
462 stable environments (Table 1). The *Porosira* gp and *T. antarctica* are associated with an
463 earlier sea-ice advance in autumn and lower temperature (Table 1; Fig.4; Table S4). These
464 results agree well with ecological preferences of those diatoms, which are considered as
465 biological indicators of early sea-ice freezing in autumn (Table 1; Note S1). However, in our
466 study the *Porosira* gp is linked to a longer ice-free season than *T. antarctica* is (Fig.4; Table
467 S4). These results contradict paleoecological inferences on these species whereby *P. glacialis*
468 has been associated with slightly longer annual sea-ice cover relative to *T. antarctica* (Pike et
469 al., 2009), maybe because these studies did not separate the two varieties of *T. antarctica*.

470 Our observations support the use of the Open Water gp, *F. kerguelensis*, Ti and [HBI:3] as
471 indicators of the lengthening of ice free conditions in paleoclimate studies (Table 1). Our
472 results are generally in line with the known environmental conditions of these proxies
473 occurrence (Table 1; Note S1), as along with *Porosira* gp and *T. antarctica*, these proxies have
474 been attributed to more open conditions in the Mertz Glacier Polynya area during periods with
475 reinforced easterly wind conditions (Campagne et al., 2015). The lengthening of the ice free
476 season results from early sea-ice retreat, probably due to the development of the DDU
477 polynya (Arrigo et al. 2003) during the early spring-summer period. Indeed, the concomitant
478 presence of the *Porosira* gp and *T. antarctica* indicate early sea-ice regrowth as a response to
479 an easterly wind field (Table 1) that has been shown to weaken the northward transport of sea
480 ice in the region, thus increasing sea-ice conditions in autumn (Massom et al., 2003; 2009).
481 This suggests that *T. antarctica* and the *Porosira* gp are good indicators for autumnal sea-ice
482 dynamics forced by atmospheric variability.

483

484 • **Katabatic winds and coastal polynya**

485 Southerly winds are of katabatic origin in our study area (Wendler et al., 1997; Note S2). A
486 dominant southerly wind component is conducive to a delayed spring sea-ice retreat and late
487 autumn freezing, higher SIC from November to March, and to some extent, a shortened ice-
488 free season in the study area (Note S2). Indeed, strong katabatic winds break the fast ice along
489 the coast, leading to enhanced open water conditions and to the formation of a coastal polynya
490 constrained to the coastline (Vaillancourt et al., 2003; Massom et al., 2009; Riaux Gobin et
491 al., 2013). However at the core site, the pack ice would be present due to a reduced fast-ice

492 buttress and the increasing northward transport of the pack ice under strong southerly winds
493 (Massom et al., 2009). Under such environmental conditions, the sedimentary response shown
494 by the PCA indicates increasing abundances of the CRS gp and Zr/Rb that are strongly linked
495 to F1- (Fig. 4). Their response to katabatic wind events is probably through the opening of a
496 coastal polynya (Note S2). In addition, although the CRS gp shows no relation with SIC
497 parameters, this group is associated to a strong wind speed (0,364; Table S4) over the ice-free
498 season, in agreement with the environmental interpretation of the species (Note S1). In
499 contrast, Zr/Rb is closely associated with increasing SIC over the ice-free season in addition
500 to a delayed sea-ice retreat (Table S4).

501 Enhanced polynya activity along the coast has been shown to coincide with a deep mixed
502 layer and high Chl a levels (Vaillancourt et al., 2003; Riaux Gobin et al., 2013). Stronger
503 vertical mixing may increase nutrient availability, favouring the rapid development of the
504 *Chaetoceros Hyalochaete* spp. Spore formation may occur through deep mixing of vegetative
505 cells under the photic zone or nutrient depletion when winds weaken. Northward lateral
506 advection of surface production from the coast to the study area may explain the occurrence
507 of CRS gp along with more sea ice at the core site. Continuous sea-ice formation in the
508 coastal polynya may favour brine production and subsequently, stronger bottom currents,
509 leading to the observed Zr/Rb high values. However changes in the phase relationship
510 between relative abundances of the CRS gp and Zr/RB content over the last 40 years argue for
511 periodic decoupling between polynya activity and katabatic winds. We propose that CRS are
512 strongly linked to katabatic wind pulses and rapid stratification/mixing events while Zr/Rb is
513 more directly linked to polynya activity (and bottom water velocity) that responds to windy
514 conditions (Table 1). Under southerly winds both high values CRS and Zr/Rb are expected
515 while under strong south to easterly winds lower CRS abundances but still high ZR/Rb values
516 are expected (Table 1).

517

518 **6 Conclusion**

519 Investigation of annual to interannual relationships between diatom communities, diatom
520 specific biomarkers and major element abundances in connection with meteorological
521 parameters shows that the relevance and use of some proxies (1) may be characteristic of the
522 study area (e.g. CRS gp assemblage), or (2) differ slightly from previous long-term studies
523 (e.g. *F. cylindrus*). Indeed, at such a fine scale, the distribution of the sea-ice related proxies

524 in sediments highlights complex relationships between the biota and sea-ice concentration,
525 dynamics, cover structure and origin, constrained by the wind pattern. Our results therefore
526 attest for the importance of the origin and nature of the sea-ice in the sedimentary distribution
527 of sea-ice proxies. A clear and unambiguous distinction of sea-ice type through a finer
528 satellite study in the region (e.g. MODIS satellite imagery) would greatly help to assess and
529 better constrain such relationships. However, we note that the complex inter-relations
530 between winds and sea ice should be alleviated at longer time scales when large atmospheric
531 and ocean temperatures changes become preponderant. On the other hand, in our study area,
532 open ocean related proxies seem to be primarily connected to the length of the growing
533 season thus agreeing well with previously published regional to-large scale studies. Polynya
534 activity may be inferred from variations in the Zr/Rb ratio values. Monitoring the sedimentary
535 signal formation in surface water, its export throughout the water column and burial in deep-
536 sea sediments are necessary to understand the regional behaviour of the proxies commonly
537 constrained via synoptic studies. Other high-resolution and longer timescale reconstructions
538 are required to refine our understanding of the ice-ocean-atmosphere interactions and system
539 feedbacks.

540

541 **Acknowledgements**

542 This research was funded by the ERC StG ICEPROXY project (203441), the ANR CLIMICE
543 project and FP7 Past4Future project (243908). The CNRS (Centre National de la Recherche
544 Scientifique) and the FRQNT (Fonds de recherche du Québec – Nature et technologies)
545 provided the student fellowship. The French Polar Institute provided logistical support for
546 sediment and data collection (IPEV projects 452 & 1010). This is ESF PolarClimate
547 HOLOCLIP contribution n°24 and Past4Future contribution n°83. The authors thank Johan
548 Etourneau and Emmanuelle Sultan for sample collection. The authors thank Debra
549 Christiansen-Stowe and Julie Sansoulet for logistical and administrative assistance.

550

551 **Author contributions**

552 X. C. & G. M. designed the study and P.C. carried it out. O.T. performed diatom extraction
553 and XRF analyses; P.C. performed diatom census counts and PCA analyses; M-N. H.

554 extracted daily sea-ice concentrations; S. S. performed ^{210}Pb analyses and developed the age
555 model of the core; P.C. prepared the manuscript with contributions from all co-authors.
556

- Adolphs, U. and Wendler, G.: A pilot study on the interactions between katabatic winds and polynyas at the Adelie Coast, eastern Antarctica, *Ant. Sci.*, 7, 307-314, 1995.
- Armand, L. K., Crosta, X., Romero, O., and Pichon, J.-J.: The biogeography of major diatom taxa in Southern Ocean sediments: 1. Sea ice related species, *Palaeogeogr. Palaeoclimatol.*, 223, 93-126, 2005.
- Arrigo, K. R. and van Dijken, G. L.: Phytoplankton dynamics within 37 Antarctic coastal polynya systems, *J. Geophys. Res.*, 108, 3271, 2003.
- Beans, C., Hecq, J. H., Koubbi, P., Vallet, C., Wright, S., and Goffart, A.: A study of the diatom-dominated microplankton summer assemblages in coastal waters from Terre Adélie to the Mertz Glacier, East Antarctica (139°E-145°E), *Pol. Bio.*, 31, 1101-1117, 2008.
- Campagne, P., Crosta, X., Houssais, M. N., Swingedouw, D., Schmidt, S., Martin, A., Devred, E., Capo, S., Marieu, V., Closset, I., and Masse, G.: Relative role of glacial ice and atmospheric forcing on the Mertz Glacier Polynya over the past 250 years, *Nat. Comm.*, 6, 6642, 2015.
- Cavalieri, D. J., St. Germain, K., and Swift, C. T.: Reduction of weather effects in the calculation of sea ice concentration with the DMSP SSM/I, *J. Glaciol.*, 41, 455-464, 1995.
- Collins, L. G., Allen, C. S., Pike, J., Hodgson, D. A., Weckström, K., and Massé, G.: Evaluating highly branched isoprenoid (HBI) biomarkers as a novel Antarctic sea-ice proxy in deep ocean glacial age sediments, *Quaternary Sci. Rev.*, 79, 87-98, 2013.
- Crosta, X. and Koc, N.: Diatoms: From micropaleontology to isotope geochemistry, in: *Methods in Late Cenozoic Paleooceanography*, edited by: Hilaire-Marcel, C. and de Vernal, A., Elsevier, Amsterdam, the Netherlands, 327-369, 2007.
- Crosta, X., Sturm, A., Armand, L., and Pichon, J. J.: Late Quaternary sea ice history in the Indian sector of the Southern Ocean as recorded by diatom assemblages, *Mar. Micropaleontol.*, 50, 209-223, 2004.
- Crosta, X., Romero, O., Armand, L. K., and Pichon, J.-J.: The biogeography of major diatom taxa in Southern Ocean sediments: 2. Open ocean related species, *Palaeogeogr. Palaeoclimatol.*, 223, 66-92, 2005.
- Defelice, D. R. and Wise, S. W.: Surface lithofacies, biofacies, and diatom diversity patterns as

models for delineation of climatic change in the southeast Atlantic Ocean, *Mar. Micropaleontol.*, 6, 29-70, 1981.

Denis, D., Crosta, X., Zaragosi, S., Romero, O., Martin, B., and Mas, V.: Seasonal and subseasonal climate changes recorded in laminated diatom ooze sediments, Adelie Land, East Antarctica, *Holocene*, 16, 1137-1147, 2006.

Dinniman, M. S., Klinck, J. M., and Hofmann, E. E.: Sensitivity of circumpolar deep water transport and ice shelf basal melt along the west Antarctic Peninsula to changes in the winds, *Amer. Meteor. Soc.*, 25, 2012.

Escutia, C. and Party, S. S.: Integrated Ocean drilling Program Expedition 318 Preliminary Report, Integrated Ocean drilling Program Management International, Inc. for the Integrated Ocean Drilling Program, 101 pp., 2010.

Escutia, C., Warnke, D., Acton, G. D., Barcena, A., Burckle, L., Canals, M., and Frazee, C. S.: Sediment distribution and sedimentary processes across the Antarctic Wilkes Land margin during the Quaternary, *Deep-Sea Res, Pt. II*, 50, 1481-1508, 2003.

Fleury, S., Martinez, P., Crosta, X., Charlier, K., Billy, I., Hanquiez, V., ... & Schneider, R. R.: Pervasive multidecadal variations in productivity within the Peruvian Upwelling System over the last millennium, *Quat. Sci. Rev.*, 125, 78-90, 2015.

Gersonde, R. and Zielinski, U.: The reconstruction of late Quaternary Antarctic sea-ice distribution - the use of diatoms as a proxy for sea-ice, *Palaeogeogr. Palaeoclimatol.*, 162, 263-286, 2000.

Giles, A. B., Massom, R. A., and Lytle, V. I.: Fast ice distribution in East Antarctica during 1997 and 1999 determined using RADARSAT data, *J. Geophys. Res.-Oceans*, 113, C02S14, doi:10.1029/2007JC004139, 2008.

Hasle, G. R.: An analysis of the phytoplankton of the Pacific Southern Ocean: abundance, composition, and distribution during the Bratigg Expedition, 1947-1948, *Univ.-Forl*, 1969.

Heil, P.: Atmospheric conditions and fast ice at Davis, East Antarctica: A case study, *J. Geophys. Res.-Oceans*, 111, C05009, doi:10.1029/2005JC002904, 2006.

Holland, P. R. and Kwok, R.: Wind-driven trends in Antarctic sea-ice drift, *Nat. Geosci.*, 5, 872-875, 2012.

- Jacobs, S.: Bottom water production and its links with the thermohaline circulation, *Ant. Sci.*, 16, 427-437, 2004.
- Kang, S.-H. and Fryxell, G. A.: *Fragilariopsis cylindrus* (Grunow) Krieger: The most abundant diatom in water column assemblages of Antarctic marginal ice edge zones, *Pol. Biol.*, 12, 609-627, 1992.
- König-Langlo, G., King, J. C., and Pettré, P.: Climatology of the three coastal Antarctic stations Dumont d'Urville, Neumayer, and Halley, *J. Geophys. Res.*, 103, 10, 935-10 946, 1998.
- Lacarra, M., Houssais, M. N., Herbaut, C., Sultan, E., and Beauverger, M.: Dense shelf water production in the Adélie Depression 2004-2012: Impact of the Mertz glacier calving, *J. Geophys. Res.*, 119, 5203-5220, 2014.
- Leventer, A.: Modern distribution of diatoms in sediments from the Georges V coast, Antarctica, *Mar. Micropaleontol.*, 19, 315-332, 1992.
- Leventer, A., Dunbar, R. B., and DeMaster, D. J.: Diatom evidence for late Holocene climatic events in Granite Harbor, Antarctica. *Paleoceanography*, 8, 3, 373-386, 1993.
- Maddison, E. J., Pike, J., Leventer, A., Dunbar, R., Brachfeld, S., Domack, E. W., Manley, P., and McClennen, C.: Post-glacial seasonal diatom record of the Mertz Glacier Polynya, East Antarctica, *Mar. Micropaleontol.*, 60, 66-88, 2006.
- Maddison, E. J., Pike, J., and Dunbar, R.: Seasonally laminated diatom-rich sediments from Dumont d'Urville Trough, East Antarctic Margin: Late-Holocene Neoglacial sea-ice conditions, *Holocene*, 22, 857-875, 2012.
- Massé, G., Belt, S. T., Crosta, X., Schmidt, S., Snape, I., Thomas, D. N., and Rowland, S. J.: Highly branched isoprenoids as proxies for variable sea ice conditions in the Southern Ocean, *Ant. Sci.*, 23, 487-498, 2011.
- Massom, R. A., Harris, P. T., Michael, K. J., and Potter, M. J.: The distribution of formative processes of latent heat polynyas in East Antarctica, *Ann. Glaciol.*, 27, 420-426, 1998.
- Massom, R. A., Eicken, H., Haas, C., Jeffries, M. O., Drinkwater, M. R., Sturm, M., Worby, A. P., Wu, X., Lytle, V. I., Ushio, S., Morris, K., Reid, P. A., Warren, S. G., and Allison, I.: Snow on Antarctic sea ice, *Rev. Geophys.*, 39, 413-445, 2001.
- Massom, R. A., Jacka, K., Pook, M. J., Fowler, C., Adams, N., and Bindoff, N.: An anomalous

- late season change in the regional sea ice regime in the vicinity of the Mertz Glacier Polynya, East Antarctica, *J. Geophys. Res.-Oceans*, 108, 3212, doi:10.1029/2002JC001354, 2003.
- Massom, R. A., Hill, K., Barbraud, C., Adams, N., Ancel, A., Emmerson, L., and Pook, M. J. Fast ice distribution in Adélie Land, East Antarctica: interannual variability and implications for emperor penguins *Aptenodytes forsteri*, *Mar. Ecol.-Prog. Ser.*, 374, 243-257, 2009.
- Meredith, M. P.: Oceanography: Replenishing the abyss, *Nat. Geosci.*, 6, 166-167, 2013.
- Migeon, S., Weber, O., Faugères, J.-C., and Saint-Paul, J.: SCOPIX: a new X-ray imaging system for core analysis, *Geo-Mar. Lett.*, 18, 251-255, 1999.
- Migeon, S., Weber, O., Faugères, J.-C. and Saint-Paul, J.: SCOPIX : a new X-ray imaging system for core analysis, *Geo-Mar. Lett.*, 18, 251-255, 1999.
- Parish, T. R. and Bromwich, D. H.: Reexamination of the near-surface airflow over the Antarctic continent and implications on atmospheric circulations at high southern latitudes*, *Mon. Weather Rev.*, 135, 1961-1973, 2007.
- Périard, C. and Pettré, P.: Some aspects of the climatology of Dumont d'Urville, adélie land, Antarctica, *Int. J. Climatol.*, 13, 313-328, 1993.
- Pike, J., Crosta, X., Maddison, E. J., Stickley, C. E., Denis, D., Barbara, L., and Renssen, H.: Observations on the relationship between the Antarctic coastal diatoms *Thalassiosira antarctica* Comber and *Porosira glacialis* (Grunow) Jørgensen and sea ice concentrations during the late Quaternary, *Mar. Micropaleontol.*, 73, 14-25, 2009.
- Presti, M., De Santis, L., Busetti, M., and Harris, P. T.: Late Pleistocene and Holocene sedimentation on the George V Continental Shelf, East Antarctica, *Deep-Sea Res. Pt. II*, 50, 1441-1461, 2003.
- Rathburn, A.E., Pichon, J.J., Ayress, M.A., De Deckker, P.: Microfossil and stable isotope evidence for changes in Late Holocene palaeoproductivity and palaeoceanographic conditions in the Prydz Bay region of Antarctica, *Palaeogeog., Palaeoclim., Palaeoecol.*, 131 (3e4), 485e510, 1997.
- Riaux-Gobin, C., Romero, O. E., Coste, M., and Galzin, R.: A new *Cocconeis* (Bacillariophyceae) from Moorea Island, Society Archipelago, South Pacific Ocean with distinctive valvocopula morphology and linking system, *Bot. Mar.*, 56, 339-356, 2013.
- Rintoul, S. R.: On the origin and influence of Adélie land bottom water, in: *Ocean, Ice, and*

- Atmosphere: Interactions at the Antarctic Continental Margin, edited by: Jacobs, S. and Weiss, R., American Geophysical Union, Washington, D. C., 75, 151-171, 1998.
- Robbins, J. A., and Edgington, D. N.: Determination of recent sedimentation rates in Lake Michigan using Pb-210 and Cs-137, *Geoch et Cosmoch Acta*, 39, 3, 285-304, 1975.
- Sambrotto, R. N., Matsuda, A., Vaillancourt, R., Brown, M., Langdon, C., Jacobs, S. S., and Measures, C.: Summer plankton production and nutrient consumption patterns in the Mertz Glacier Region of East Antarctica, *Deep-Sea Res. Pt. II*, 50, 1393-1414, 2003.
- Schmidt, S. and De Deckker, P.: Present-day sedimentation rates on the southern and southeastern Australian continental margins, *Aust. J. Earth Sci.*, 62, 143-150, 2015.
- Sinningh  Damst , J. S., Muyzer, G., Abbas, B., Rampen, S. W., Mass , G., Allard, W. G., Belt, S. T., Robert, J. M., Rowland, S. J., Moldowan, J. M., Barbanti, S. M., Fago, F. J., Denisevich, P., Dahl, J., Trindade, L. A. F., and Schouten, S.: The rise of the Rhizosolenoid diatoms, *Science*, 304, 584-587, 2004.
- Smik, L., Belt, S. T., Lieser, J. L., Armand, L. K., & Leventer, A.: Distributions of highly branched isoprenoid alkenes and other algal lipids in surface waters from East Antarctica: Further insights for biomarker-based paleo sea-ice reconstruction, *Organ. Geochem.*, 95, 71-80, 2016.
- Smith, M. B., Labat, J. P., Fraser, A. D., Massom, R. A., and Koubbi, P.: A GIS approach to estimating interannual variability of sea ice concentration in the Dumont d'Urville Sea near Terre Ad lie from 2003 to 2009, *Pol. Sci.*, 5, 104-117, 2011.
- Stammerjohn, S. E., Martinson, D. G., Smith, R. C., Yuan, X., and Rind, D.: Trends in Antarctic annual sea ice retreat and advance and their relation to El Ni o-Southern Oscillation and Southern Annular Mode variability, *J. Geophys. Res.*, 113, C03S90, 2008.
- Vaillancourt, R. D., Sambrotto, R. N., Green, S., and Matsuda, A.: Phytoplankton biomass and photosynthetic competency in the summertime Mertz Glacier Region of East Antarctica, *Deep-Sea Res. Pt. II*, 50, 1415-1440, 2003.
- Wang, Z., Turner, J., Sun, B., Li, B., and Liu, C.: Cyclone-induced rapid creation of extreme Antarctic sea ice conditions, *Scientific Reports*, 4, 5317, doi:10.1038/srep05317, 2014.
- Wendler, G., Stearns, C., Weidner, G., Dargaud, G., and Parish, T.: On the extraordinary katabatic winds of Ad lie Land, *J. Geophys. Res.-Atmos.*, 102, 4463-4474, 1997.

Williams, G. D. and Bindoff, N. L.: Wintertime oceanography of the Adélie depression, *Deep-Sea Res. Pt. II*, 50, 1373-1392, 2003.

Williams, G. D., Bindoff, N. L., Marsland, S. J., and Rintoul, S. R.: Formation and export of dense shelf water from the Adélie Depression, East Antarctica, *J. Geophys. Res.*, 113, C04039, doi:10.1029/2007JC004346, 2008.

Zhai, M., Li, X., Hui, F., Cheng, X., Heil, P., Zhao, T. and Liu, J.: Sea-ice conditions in the Adélie Depression, Antarctica, during besetment of the icebreaker RV Xuelong, *Ann. Glaciol.*, 56(69), 160, 2015.

Zielinski, U. and Gersonde, R.: Diatom distribution in Southern Ocean surface sediments (Atlantic sector): Implications for paleoenvironmental reconstructions, *Palaeogeogr. Palaeoclimatol.*, 129, 213-250, 1997.

559 Table 1. Summary of the relationships between sedimentary proxies and
 560 environmental conditions.

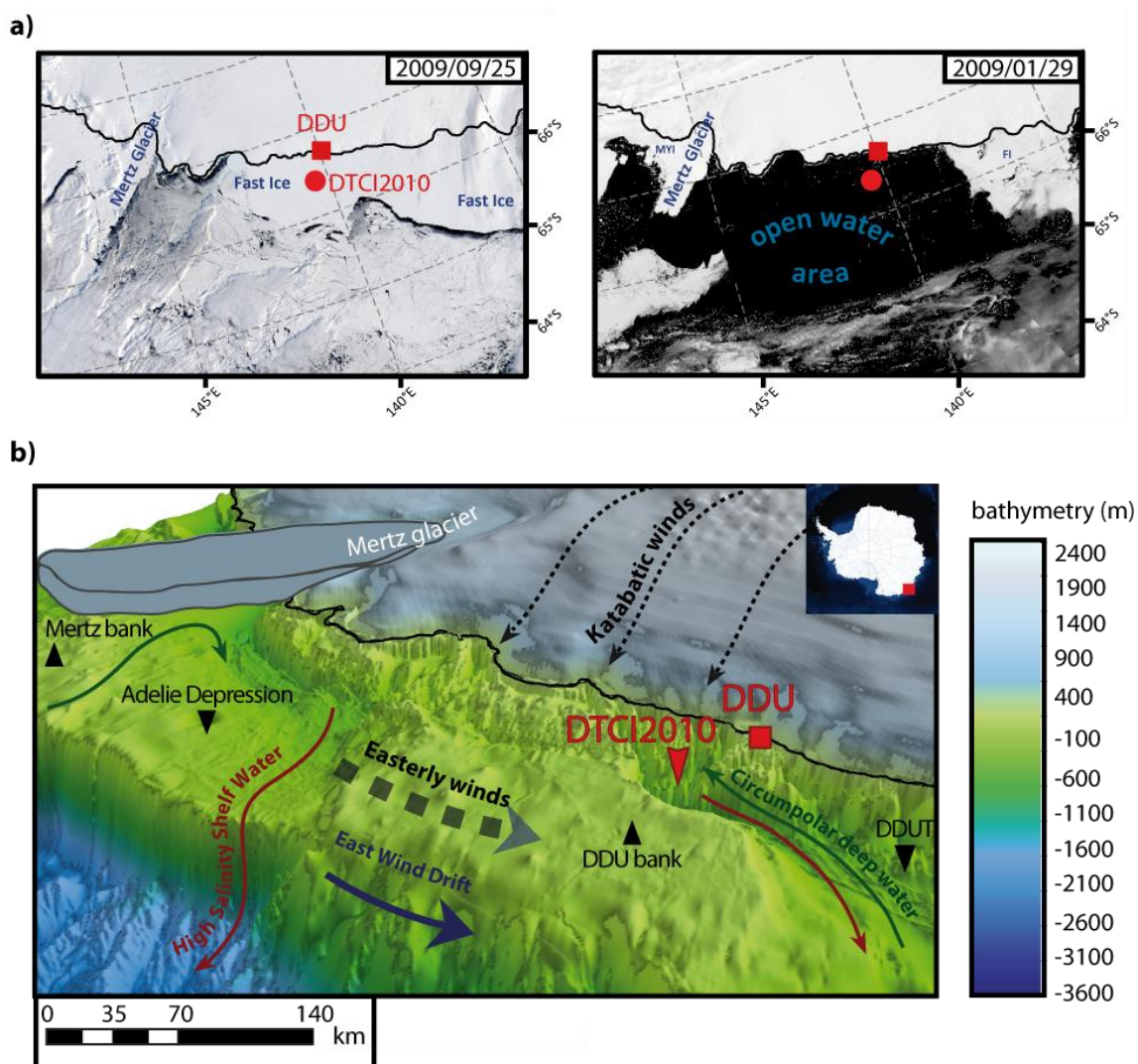
PROXY/GROUP IDENTIFIED IN CORE DTCI2010	KNOWN ECOLOGY (LITERATURE)	ENVIRONMENTAL RELATIONSHIPS OFF ADÉLIE LAND
<i>F. cylindrus</i>	Spring sea-ice covered/sea-ice stratified waters	Compacted pack ice in spring by northerly winds (“warm” sea ice), sea-ice stratified waters
[HBI:2], [HBI:2]/[HBI:3]	Spring sea-ice environment	Compacted pack ice or fast ice in spring by westerly winds (cold sea ice)
Banquisia gp(<i>N. directa</i> , <i>N. glaciei</i> , <i>Synedra</i> spp, <i>Ephemera</i> spp)	Spring sea-ice conditions	No clear pattern
<i>F. obliquecostata</i>	Surface melt pools, sea-ice covered waters in summer	No clear pattern
<i>E. antarctica</i>	Ubiquist, open conditions, melting glacial ice	Onshore winds increase spring-summer sea ice (short ice free season, delayed sea-ice retreat)
<i>Fragilariopsis</i> summer gp (<i>F. ritscheri</i> , <i>F. sublinearis</i>)	Summer sea-ice edge environment, melted waters	No clear pattern
<i>T. antarctica</i>	Open water conditions in summer-autumn, slush and wave-exposed shore ice environment	Summer open water conditions but icy autumn conditions (early sea-ice advance) induced by easterly winds
<i>Porosira</i> gp (<i>P. glacialis</i> , <i>P. pseudodenticulata</i>)	Relative open water conditions in summer, slush and wave-exposed shore ice environment, icy autumn and early sea-ice advance	Summer open water conditions but icy autumn conditions (early sea-ice advance) induced by easterly winds
<i>F. kerguelensis</i>	Open water, ice free conditions during summer	Summer open water conditions (early sea-ice retreat, long ice free

		season) induced by easterly winds
Open water gp (<i>T. lentiginosa</i> , <i>T. oliverana</i> , <i>T. trifulta</i> , <i>T. gracilis</i> , <i>T. tumida</i> , <i>Coscinodiscus</i> spp, <i>A. actinochilus</i> , <i>S. microtrias</i>)	Open water, ice free conditions during summer	Summer open water conditions (early sea-ice retreat, long ice free season) induced by easterly winds
[HBI:3]	Marginal Ice Zone, open water, ice-free conditions during summer	Summer open water conditions (early sea-ice retreat) induced by easterly to northerly winds
<i>Rhizosolenia</i> gp (<i>Rhizosolenia</i> spp, <i>R. antennata semispina</i> , <i>Proboscia</i> spp, <i>P. truncata</i> and <i>P. inermis</i>)	Open conditions in summer/autumn, stratified oligotrophic waters	No clear trend with sea-ice conditions, stable summer surface waters induced by northerly winds
<i>Thalassiotrix</i> gp (<i>Tx. antarctica</i> , <i>T. reinboldii</i>)	Open conditions in autumn, highly stable and nutrient poor water column	Summer open water conditions (early sea-ice retreat, long ice free season) induced by easterly winds
<i>F. rhombica</i>	Unconsolidated sea ice in spring, ice-free summer	Warm conditions in spring-summer, delayed ice free season (late sea-ice retreat and late sea-ice advance)
Ti	Summer open conditions favoring glacial melting	Rapid sea-ice melting in spring, warm open-water conditions in summer induced by northerly winds
Zr/Rb	Polynya environment	Coastal polynya activity under intense southerly to souht-easterly winds
CRS GP (<i>Chaetoceros Hyalochaetes</i> spp)	Rapid changes in stratification, decreasing nutrient levels	Stratification disruption at the MIZ or within polynyas by katabatic wind pulses (high wind speed)
<i>Phaeoceros</i> gp (<i>C. Phaeoceros</i> spp, <i>C. atlantica</i> , <i>C. dictyota</i>)	Open water environment	No clear pattern

<p>Benthic gp (<i>Cocconeis</i> spp, <i>Grammatophora</i> spp, <i>Trachyneis</i> spp, <i>Licmophora</i> spp, <i>Melosira solenia</i>, <i>Achnantes brevipes</i>, <i>Amphora</i> spp, <i>Diploneis</i> spp, <i>Melosira</i> <i>adelia</i>, <i>Pseudogomphonema</i> spp, <i>O. weissflogii</i>)</p>	<p>Spring wind (storm) induced mixing conditions</p>	<p>No clear pattern</p>
<p><i>Corethron</i> gp (<i>C. criophilum</i>, <i>C.</i> <i>pennatum</i>)</p>	<p>Open ocean conditions, surface mixed waters</p>	<p>No clear pattern</p>

561

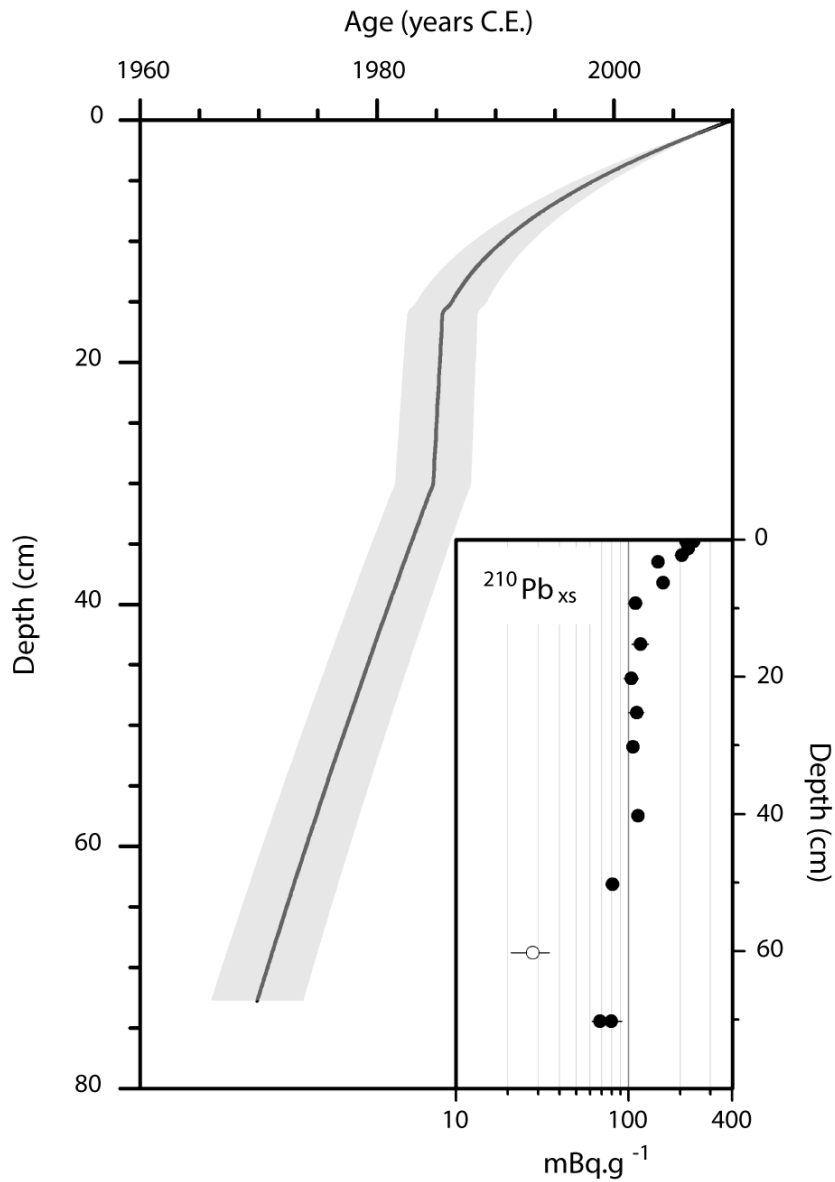
562



563

564 Figure 1. Study area. **a)** Modis satellite images of Adélie Land, showing mean sea-ice
 565 conditions from early spring to summer in the region, the location of sediment core
 566 DTCI2010 and the French research station Dumont D'Urville (DDU). **b)** Map of the study
 567 area showing the location of sediment core DTCI2010 in the Dumont D'Urville Trough
 568 (DDUT), the main glacial and topographic features, the principal water masses (solid lines)
 569 and the main wind streams (dahsed lines).

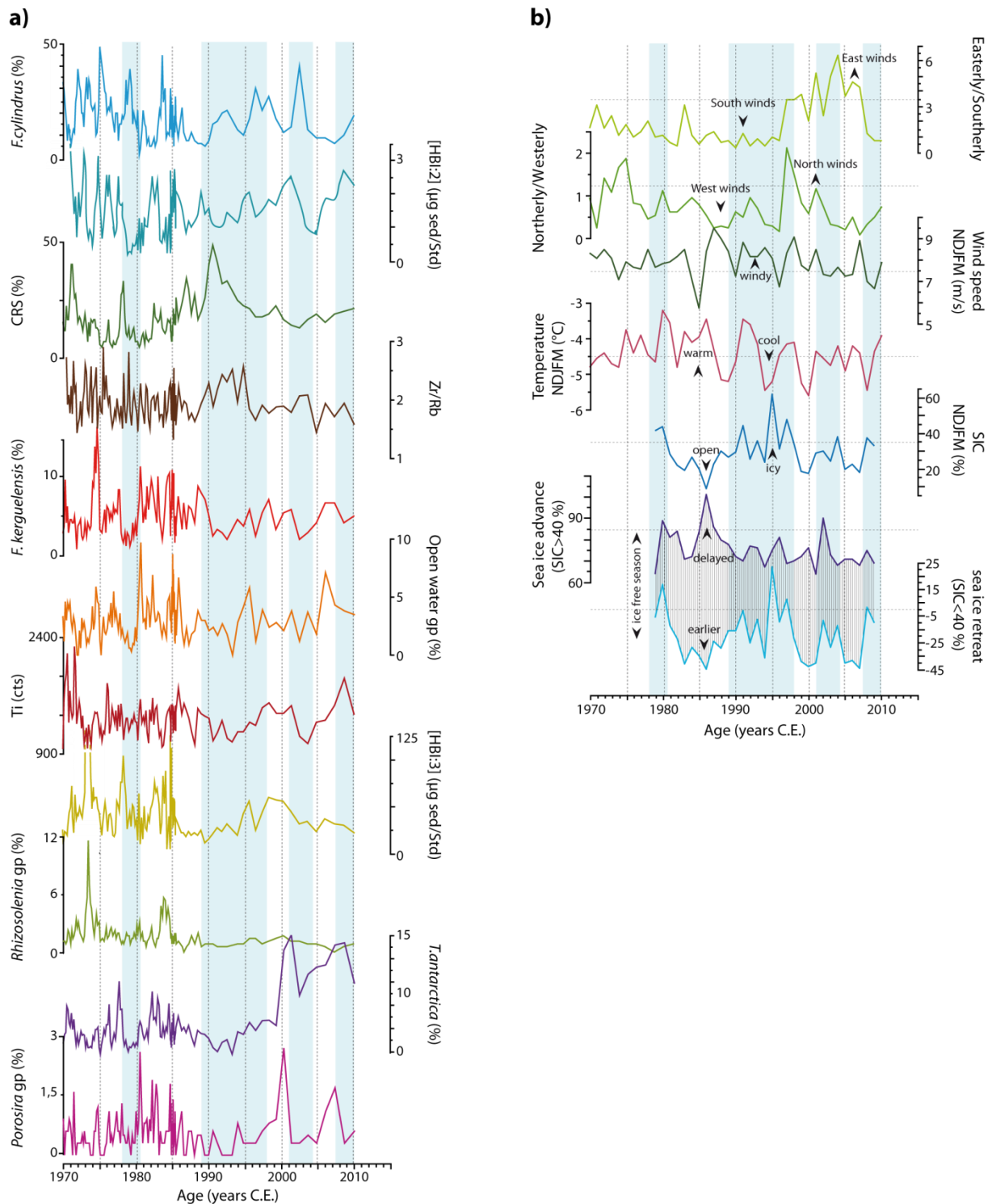
570



571

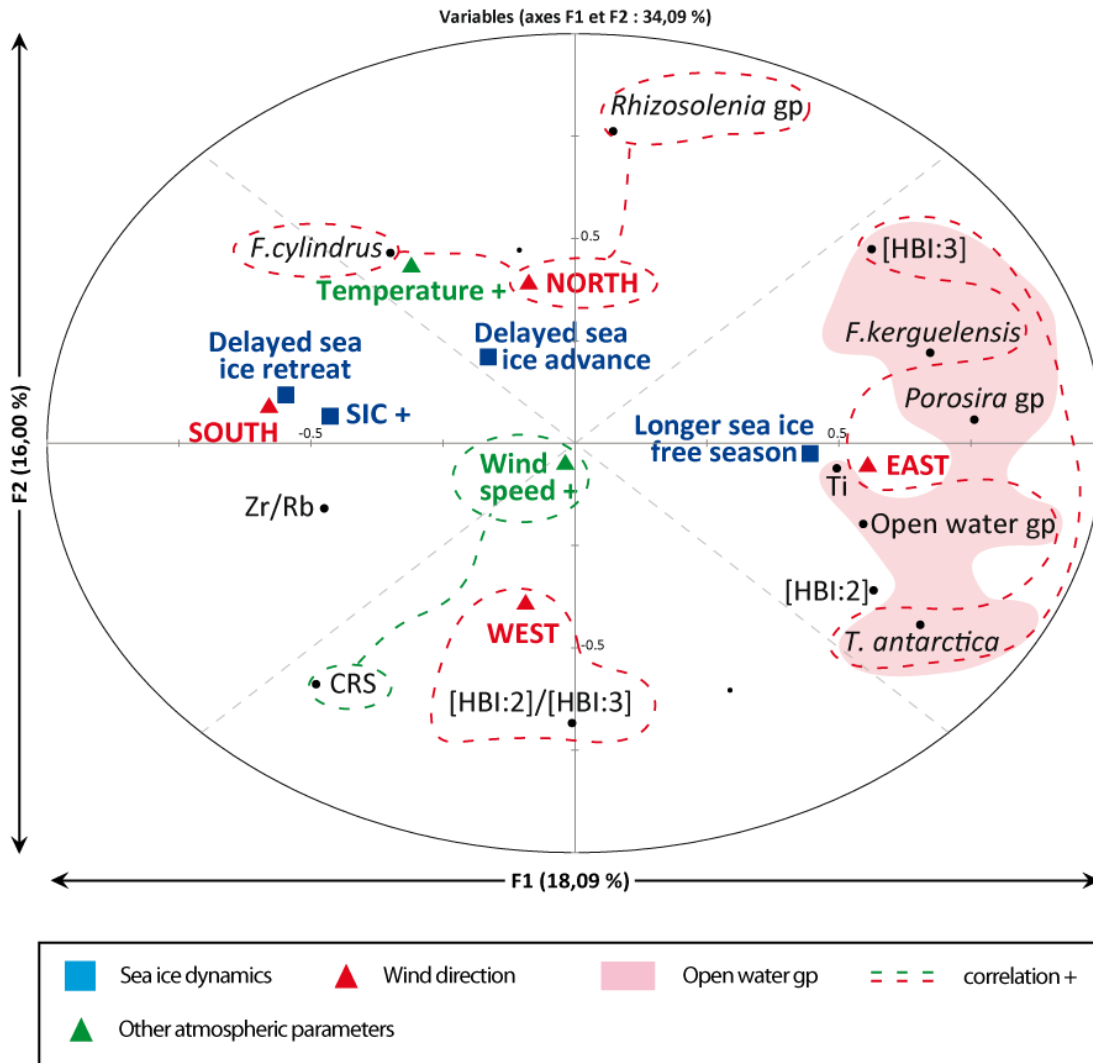
572 Figure 2. DTCI2010 chronology, based on ^{210}Pb excess ($^{210}\text{Pb}_{\text{xs}}$) and associated age-model
 573 errors (grey area). The inset corresponds to the downcore profile of $^{210}\text{Pb}_{\text{xs}}$ (error bars
 574 correspond to 1 SD).

575



576

577 Figure 3. **Part a)** Raw sedimentary records from DTIC2010 interface core over the 1970-
 578 2010 period. The blue shading indicates periods marked by increasing monitored sea-ice
 579 concentration at the core site. **Part b)** Meteorological parameters and climate index over the
 580 1970-2010 period. Daily meteorological parameters were averaged over the November to
 581 March period. Blue shaded areas mark increases of SIC.



583

584 Figure 4. PCA applied to standardized sedimentary data from the DTIC2010 core and
 585 meteorological parameters. The yearly standardized sedimentary data represent the ice-free
 586 season of the related year. Weather forecast/satellite data were averaged between November
 587 and March. F1 axis represents the sea-ice conditions linked to the predominant Easterly and
 588 Southerly winds. F2 axis represents the secondary wind directions in the study area, Northerly
 589 and Westerly winds.

590

591

592